Application of Image-Based Skin Chromophore Analysis to Cosmetics

Nobutoshi Ojima,* Syuuichi Akazaki and Kimihiko Hori
Skin Care Beauty Center, Kao Corporation, Tokyo, Japan

Norimichi Tsumura▲ and Yoichi Miyake✦
Department of Information and Image Sciences, Chiba University, Chiba, Japan

The spatial distributions of melanin and hemoglobin in human skin can be determined by image-based skin chromophore analysis including independent component analysis (ICA) of a skin color image. The separation is based on the skin color model in the optical density domain to quantify the change in the chromophores. In this paper, the analysis technique developed by Tsumura et al. was applied to many skin images, and the distribution of skin chromophores, such as melanin and hemoglobin, agreed well with the physiological knowledge. The effectiveness of cosmetic products was also evaluated by observing the changes in the amount of each chromophore. Finally a simulation to synthesize the changes in skin chromophores was performed to demonstrate its validity.

Journal of Imaging Science and Technology 48: 222–226 (2004)

Introduction

With the recent progress of various imaging systems such as multimedia, computer graphics and telemedicine systems, skin color has become increasingly important for communication, image reproduction on hardcopy and softcopy, medical diagnosis, etc.[1–4] In the cosmetics industry[5–7] also, skin color is very important because skin color communicates not only facial impression but also body and skin conditions. For this reason, in order to develop and provide cosmetics which suit skin conditions for each person, skin diagnosis and the evaluation of efficacy of skin care products have been very important. However, in case of skin tone lightening essence, which limits the production of melanin chromophore, it was very difficult to evaluate the effectiveness for each chromophore only by colorimetric values, because the values contain information on various skin chromophores such as melanin and hemoglobin at the same time. Therefore it is necessary to extract the information of each skin chromophore independently as density information, especially as a two-dimensional density distribution.

Techniques to separate melanin and hemoglobin chromophores are being developed currently. Shimada[8] and Nakai[9] estimated chromophore density from spectral reflectance of skin. Image processing techniques to estimate distribution of melanin, oxyhemoglobin and dioxyhemoglobin are also being developed using inverse Monte Carlo simulation by Okuyama et al.[10] However, since these techniques need absolute reflectance, specific lighting conditions, such as diffused lighting with integrated sphere or spatio-temporal modulation of lighting, are required.

Tsumura et al.[11] proposed a technique in which hemoglobin and melanin chromophore densities are extracted from a single skin color image using independent component analysis (ICA[12–15]) without special geometrical lighting conditions. The technique proposes a model to remove shading by a simple inverse lighting technique. Skin color distribution without shading is searched for the entire face, and the shading factor is removed by projecting the observed color onto a skin color distribution plane. Since the technique allows us to use various geometric lighting conditions, it has the capacity to expand the scope of applications to other fields such as telemedicine under various illuminations, skin-care check at cosmeticshops, facial image processing on TV commercials, etc.

In this study, we apply image-based skin chromophore analysis to cosmetics. The validity of this method for cosmetics was examined and given an explanation from several points of view of skin diagnosis and usefulness in evaluating the efficacy of cosmetic products. The beginning of the experiments in this article was already introduced in the paper by Tsumura et al.[11]; however, in this paper we will show the experiment on the aspects of cosmetics mentioned above. At first, skin of artificially generated chromophores was captured and analyzed by the Tsumura's technique to confirm the physiological validity. Secondly, it was applied to actual facial skin color images to diagnose skin conditions, such as acne. Thirdly, the efficacy of cosmetic products, especially lightening essence, was evaluated by the technique. The relative amount of melanin reduction by the lightening product was calculated, and was compared with the result of a

Original manuscript received July 11, 2003

▲ IS&T Fellow

✦ IS&T Member

* ojima.nobutoshi@kao.co.jp

Color Plates 2 through 7 are printed in the color plates section of this issue, pp. 236–238.

placebo sample. Finally, with the reference of the actual change in each chromophore density by the lightening product, a woman's facial skin images were synthesized in various density of melanin or hemoglobin chromophore.

The schematic flow in the image-based skin color analysis is shown in **Color Plate 2, p. 236**. The original photo was separated into the images of surface and body reflection[16] using polarized light.[17] The body reflection image was analyzed by the ICA technique to isolate both melanin and hemoglobin component images. By using these images, the relative density of each chromophore component was measured.

Modeling of Skin Color for ICA

In this section, we outline the technique proposed by Tsumura et al.[11] Modeling of skin color for independent component analysis (ICA) and shading removal technique by a simple inverse lighting technique is outlined step by step.

ICA is a technique that extracts the original signals from mixtures of many independent sources without *a priori* information on the sources and the process of the mixture.

The observed vector $\boldsymbol{v}(x,y)$, whose elements are not mutually independent, is defined as follows:

$$\boldsymbol{v}(x,y) = \mathbf{A}\,\boldsymbol{s}(x,y) \tag{1}$$

where $\boldsymbol{s}(x,y)$ is the source signal vector, and A is a 2 × 2 mixing matrix. By applying the ICA to the observed vector, the relative source signals are extracted without *a priori* information on these items, by assuming that original source signals are mutually independent. In performing ICA, the following equation was defined by using a separating matrix **H** and an extracted independent vector $\boldsymbol{e}(x,y)$ as follows;

$$\boldsymbol{e}(x,y) = \mathbf{H}\,\boldsymbol{v}(x,y) \tag{2}$$

Many methods for finding the separation matrix **H** have been proposed. In this study, optimization techniques based on the fixed-point method[12–15] are used to find the separation matrix **H**. Tsumura et al. described the details of the theory.[18]

A two layer skin model is used in the imaging process as shown in Fig. 1. Part of the incident light is reflected onto the surface as a Fresnel reflection, and other parts penetrate into the epidermis layer and dermis layers and are diffusely reflected. The body reflection can be written as in Eq. (3), assuming that the modified Lambert–Beer law is applicable in the skin layer for incident light. The modified Lambert–Beer law is assumed in Eq. (3):

$$L(x,y,\lambda) = \exp\{-\rho_m(x,y)\sigma_m(\lambda)l_e(\lambda) - \rho_h(x,y)\sigma_h(\lambda)l_d(\lambda)\}E(x,y,\lambda) \tag{3}$$

where λ is the wavelength, $E(x,y,\lambda)$ and $L(x,y,\lambda)$ are the spectral irradiance and spectral radiance to imaging devices, respectively, at the position (x,y) on the surface, and $\rho_m(x,y)$, $\rho_h(x,y)$, $\sigma_m(\lambda)$, $\sigma_h(\lambda)$ are the pigment densities and spectral cross-sections of melanin and hemoglobin, respectively. For the modified Lambert–Beer law,[19] $l_e(\lambda)$ and $l_d(\lambda)$ are the mean path lengths of photons in the epidermis and dermis layers, respectively. The surface reflection is removed by polarization filters in front of both the camera and the light source by using the algorithm proposed by Ojima et al.[17] Sensor response v_i $(i = R,G,B)$ from the digital camera can be obtained as follows:

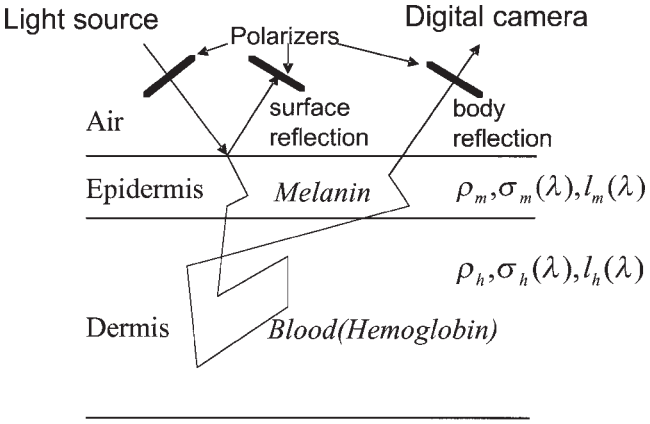

Figure 1. Schematic expression of a two-layered skin model.

$$\begin{aligned} v_i(x,y) &= c\int L(x,y,\lambda)s_i(\lambda)d\lambda \\ &= c\int\exp\{-\rho_m(x,y)\sigma_m(\lambda)l_e(\lambda) - \rho_h(x,y)\sigma_h(\lambda)l_d(\lambda)\}E(x,y,\lambda)s_i(\lambda)d\lambda \end{aligned} \tag{4}$$

where $s_i(\lambda)$ $(i = R,G,B)$ is the spectral sensitivity of the digital camera, and c is a constant value determined from the gain of the camera. If we assume the spectral sensitivity is a narrow band and can be approximated by the delta function,[20] e.g., $s_i(\lambda) = \delta(\lambda - \lambda_i)$, and if we assume that the skin is illuminated by a single color of illuminant, the spectral radiance of illuminant is separable as $E(x,y,\lambda) = p(x,y)\,\bar{E}(\lambda)$, and we can obtain the following equation from Eq. (4):

$$v_i(x,y) = c\exp\{-\rho_m(x,y)\sigma_m(\lambda)l_e(\lambda) - \rho_h(x,y)\sigma_h(\lambda)l_d(\lambda)\}p(x,y)\;\bar{E}(\lambda_i) \tag{5}$$

From the logarithm transformation of Eq. (5), we obtain the following equation by vector and matrix formulation:

$$\mathbf{v}^{\log}(x,y) = -\rho_m(x,y)\mathbf{s}_m - \rho_h(x,y)\mathbf{s}_h + p^{\log}(x,y)\mathbf{1} + e^{\log} \tag{6}$$

where,

$$\begin{aligned} \mathbf{v}^{\log} &= \left[\log\left(v_R(x,y)\right), \log\left(v_{G(x,y)}\right), \log\left(vB(x,y)\right)\right]^t, \\ \mathbf{s}_m &= \left[\sigma_m(\lambda_R)l_e(\lambda_R), \sigma_m(\lambda_G)l_e(\lambda_G), \sigma_m(\lambda_B)l_e(\lambda_B)\right]^t, \\ \mathbf{s}_h &= \left[\sigma_h(\lambda_R)l_d(\lambda_R), \sigma_h(\lambda_G)l_d(\lambda_G), \sigma_h(\lambda_B)l_d(\lambda_B)\right]^t, \\ \mathbf{1} &= \left[1,1,1\right]^t, \\ \mathbf{e}^{\log} &= \left[\log\left(E(\lambda_R)\right), \log\left(E(\lambda_G)\right), \log\left(E(\lambda_B)\right)\right]^t, \\ p^{\log}(x,y) &= \log\left(p(x,y)\right) + \log(c). \end{aligned}$$

the observed signals $\mathbf{v}^{\log}$ can be represented by the weighted linear combination of the three vectors **sm**, **sh**, **1** with the bias vector $\mathbf{e}^{\log}$, as shown in Fig. 2.

In practical application, shading on the face is caused by directional light, and this results in a wrong estimate for the density of pigment on the shaded area. Since the skin texture of color is homogeneous in the local area, the strength of shading is added to each value of skin color in 3D configuration. In order to remove shading, it is necessary to find the appropriate 2D skin color plane spanned by the absorbance vectors **sm**, **sh** and to decompose the observed skin color vector from shading directed to the vector **1**. The appropriate 2D skin plane is obtained by principal component analysis (PCA) in the range of flat portion of skin. Since the strength of

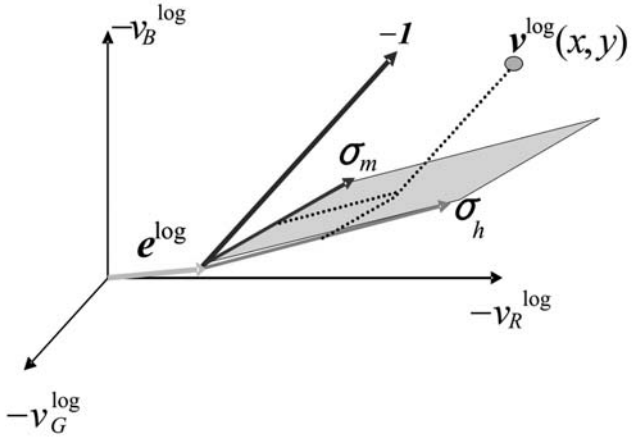

Figure 2. Schematic expression of skin color distribution in the optical density domain of three channels.

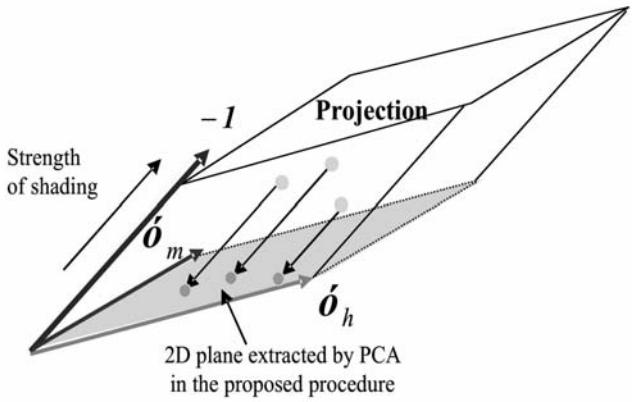

Figure 3. Projection onto the skin color plane to remove shading.

shading is directed to the **1** for any device and illuminant, the observed skin color vector $\mathbf{v}^{\log}(x,y)$ can be decomposed by projecting it onto 2D skin plane along the vector 1 (Fig. 3). The projected skin color vector $\mathbf{v}^{\text{bg}}_{\text{projection}}$ is obtained as follows;

$$\mathbf{v}^{\log} = \left[\mathbf{s}_m\ \mathbf{s}_h\ \mathbf{1}\right]\left[-\rho_m, -\rho_h, p^{\log}\right]^t + \mathbf{e}^{\log} \tag{7}$$

Rewriting, we arrive at:

$$\left[-\rho_m, -\rho_h, p^{\log}\right]^t = \left[\mathbf{s}_m\ \mathbf{s}_h\ \mathbf{1}\right]^{-1}\left(\mathbf{v}^{\log} - \mathbf{e}^{\log}\right)$$

The bias vector $\boldsymbol{e}^{\log}$ is unknown. Therefore, if we assume that the smallest value of each pigment in the skin image is zero, then $\boldsymbol{e}^{\log}$ is calculated by

$$\mathrm{e}_i^{\log} = \min\left(v_{\mathrm{i}}^{\log}(x,y)\right)$$

for each band of color. Based on the above decomposition, the shading term $p^{\log}\mathbf{1}$ is removed as follows:

$$\mathbf{v}^{\log}_{\text{projection}} = \left[\mathbf{s}_m\ \mathbf{s}_h\ 0\right]\left[\mathbf{s}_m\ \mathbf{s}_h\ \mathbf{1}\right]^{-1}\left(\mathbf{v}^{\log} - \mathbf{e}^{\log}\right) + \mathbf{e}^{\log}. \tag{8}$$

The components (**Color Plates 3(e) and 3(f), p. 236**) extracted with the shading removal technique are compared with the components without the shading removal (**Color Plate 3(b) and 3(c) p. 236**). Shading caused by the shape of the nose was removed in **Color Plate 3(e)** and **3(f), p. 236**.

Experimental Results

Analysis of Artificially Generated Chromophores

In order to confirm the physiological validity of the image-based skin chromophore technique, two practical experiments were performed on four volunteers: One was ultraviolet B (UV-B) irradiation on the arms of volunteers to identify the melanin component. The other was the application of methyl nicotinate, which is known to increase blood circulation, to the other arms for the hemoglobin component. A typical example of a volunteer has already been introduced,[11] but we show the results on four volunteers to confirm the validity and the repeatability of the technique.

A typical example is shown below. An image of the arm, where UV-B (1.5 Minimum Erythema Dose) was irradiated in local rectangular areas, was taken after two weeks by a digital camera (Nikon D1, 2,000 × 1,312 pixels). An image of the arm, where methyl nicotinate (1 mg/ml solution) was applied in a local round area, was also taken with a digital camera 30 minutes after application. These images were analyzed by the proposed method. **Color Plates 4(a)**, **4(b)**, and **Color Plate 4(c), p. 237** show the original skin image and the images of the densities for the melanin and hemoglobin components, respectively. On the other hand, **Color Plates 4(d)**, **4(e)**, and **4(f), p. 237** show the original skin image for methyl nicotinate and the images of the densities for the melanin and hemoglobin components, respectively. **Color Plate 4(b), p. 237** shows the square patterns caused the by melanin component, but the patterns did not appear in the hemoglobin component in **Color Plate 4(c), p. 237. Color Plate 4(f), p. 237** also shows the round patterns, which indicate the biological response of hemoglobin to methyl nicotinate, but there was not any response in the melanin component in **Color Plate 4(e), p. 237**. These practical experiments were performed on four Japanese volunteers (males) to confirm repeatability. Though their arms are different in shape and skin color, it was found in common that the shading of each chromophore component image was reduced and that physiological feedback of each chromophore against UV-B irradiation or application of methyl nicotinate was the same as in the typical example (**Color Plate 4, p. 237**). We can also indirectly conclude that the approximations embedded in the imaging model above is valid in our applications.

Additionally, the difference of melanin density between the two regions indicated as no. 1 and no. 2 in **Color Plates 5(a), p. 237**, corresponding to the areas without and with UV-B irradiation, was compared with the colorimetric values (CIE 1976L*a*b*). It was indicated that an increase of melanin alone had a strong effect on the decrease of L* and some effect on the increase of a*, b* (**Color Plate 5(c), p. 237**). For this reason, L* was historically used as an indicator for degree of skin tanning in the cosmetic field. However, since a change in hemoglobin density also has an effect on the change of L*, it is not sufficient to quantify the change in melanin density only. We therefore introduce the result of measuring the change in melanin density, using the proposed analyzing technique discussed below.

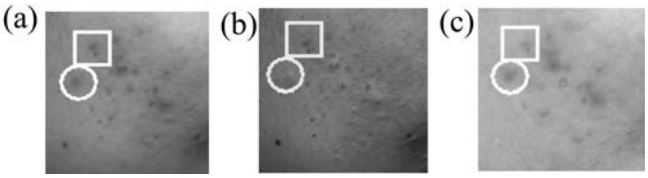

Figure 4. Analysis of acne on actual facial skin: (a) original image, (b) melanin component, and (c) hemoglobin component.

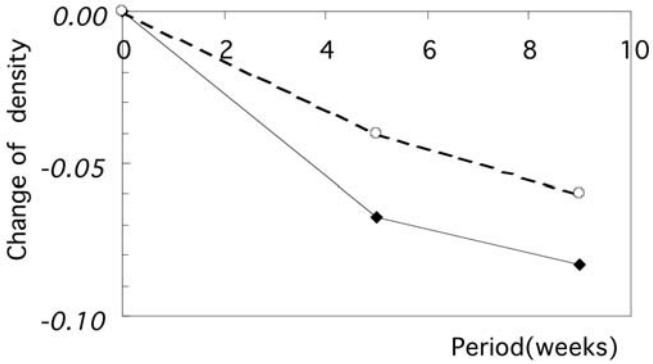

Figure 5. Relative changes in melanin density during the nine weeks the lightening essence was applied. Dotted line: placebo group. Solid line: sample group

Analysis of Facial Skin

The proposed analysis was applied to actual facial images. The first example is skin congested with blood (**Color Plates 6, p. 238**). The blood congestion appeared clearly in the hemoglobin component image (**Color Plates 6(c), p. 238**) in separation of melanin pigmentation around pores, shown in the melanin component image ((**Color Plates 6(b), p. 238**).

As another example, an image of facial skin with acne was taken and analyzed (Fig. 4). Both square and circular area in Fig. 4 indicate acne papules. In the original image (Fig. 4(a)), both acne papules are similar to each other. The extracted hemoglobin component image (Fig. 4(c)) shows there were rashes in both areas, but only melanin pigmentation occurred in the square area (Fig. 4(b)). In consequence, the acne papule in the square area was concluded to be an acne scar. This result shows that two acne papules which are similar in the original image can be disciminated by comparing the chromophore component, especially the melanin component in this case.

As described above, it was found that the proposed analysis showed the skin condition clearly and identified the condition. The analysis is expected to be useful for diagnosis in the fields of cosmetics, dermatology, telemedicine and others.

Evaluating Efficacy of Cosmetic Products

In order to evaluate the effectiveness of cosmetic products such as lightening essence, facial skin color images of 39 female subjects were captured periodically and analyzed. A cosmetic product, which is useful for lightening skin color, was applied to their faces every day for nine weeks. Subjects were separated into two groups. One was a sample group and the other was a placebo group, and each group used a sample with or without lightening essence, respectively. Figure 5 shows the change in melanin densities from the beginning (week 0). It was confirmed that the melanin densities of the sample group (19 females) decreased on average more and faster than those of the placebo group (10 females). The change in melanin density decreased during the nine weeks, by about 0.1 (Fig. 5).

Skin Color Synthesis

In order to understand and experience the changes of each chromophore component, we made a simulator to synthesize the various facial skin color images by changing the extracted chromophore components. A simulation was performed by reversing the analysis process shown in **Color Plate 2, p. 236**. As examples, synthesized images of a woman's face were made by uniformly decreasing and increasing the hemoglobin and melanin components, shown in **Color Plate 7, p. 238**. The center image is of the original skin color. Each column of images indicates the decrease and increase of the amount of hemoglobin. From left to right, the amount of hemoglobin is decreased or increased by –0.2, 0.0, 0.2. These values are relative values since the absorbance vector is normalized in the process. Each row of the images indicates the decrease and increase of the amount of melanin. From left to right, the amount of melanin is decreased or increased by –0.2, 0.0, 0.2. The step of variation in melanin densities are set at the maximum of measured density, that is double the average amount measured after nine weeks of treatment with lightening essence. Since the amount can be easily changed with a graphical user interface (GUI) with our simulation system, we can see realistic changes of facial color in real time. Though physiological feedback data from the application of a lightening essence was used for simulation, it will be necessary to collect various data of physiological feedback from external and internal stimuli.

Conclusions

The practical image-based skin color analysis technique worked very well to separate skin chromophore components from a facial skin image.

The physiological validity of the technique was confirmed by analyzing skin of artificially generated melanin or hemoglobin.

It was indicated that the chromophore component images were very useful to classify skin conditions, such as acne particles which seem to be similar to the original images. There are several skin conditions in which the main cause of skin color pattern are very difficult to determine, such as dark circles around the eyes. The image-based skin color analysis technique will be very useful, because it extracts melanin, hemoglobin and shading information in separate channels but at the same time.

The effectiveness of a cosmetic product (lightening essence) was quantitatively evaluated by observing the changes in the amount of extracted melanin chromophores. A woman's facial image was simulated by using the measured physiological feedback of melanin from this experiment. In order to achieve adequate and realistic physiological simulations, we have to collect much more physiological feedback data.

However, physiological reality is more complex in the skin than assumed herein.[21] Hemoglobin has two types of state: oxyhemoglobin and dioxyhemoglobin. The spectral absorbance is different for each other, and the ratio between them will change spatially on a large area of skin image or in an area of skin disease. It is also known that there are at least two common varieties of melanin. There are also other pigments in the skin. These

may introduce errors in the analysis of skin images by the proposed technique. Further research should be conducted to clarify the limitation and robustness of the techniques.

Acknowledgment. We are grateful for the experimental cooperation of Mr. T. Tsugita, Ms. Y. Iba, Ms. N. Okiyama, Dr. K. Higuchi, Dr. N. Komeda.

References

1. F. H. Imai, N. Tsumura, H. Haneishi, and Y. Miyake, Principal component analysis of skin color and its application to colorimetric color reproduction on CRT display and hardcopy, *J. Imaging Sci. Technol.* **40,** 422 (1996).
2. Y. Miyake, *Analysis and evaluation of digital color images*, University of Tokyo Press, 2000 (ISBN4-13-061116-x), p. 147.
3. Y. Yokoyama, N. Tsumura, H. Haneishi, Y. Miyake, J. Hayashi, and M. Saitoh, *Proc. IS&T/SID's 5th Color Imaging Conference, Color Science, Systems and Application,* IS&T, Springfield, VA, 1997, p. 169 (1997).
4. M. Yamaguchi, R. Iwama, Y. Ohya, T. Obi, N. Ohyama, and Y. Komiya, Natural color reproduction in the television system for telemedicine, *Proc. SPIE* **3031,** 482 (1997).
5. N. Ojima, O. Osanai and S. Akazaki, Image synthesis of cosmetic-applied skin based on optical properties of foundation layer, *Proc. International Congress of Imaging Science '02*, SPSTJ, Tokyo, Japan, 2002, p. 467.
6. T. Kaneko, M. Inoue, H. Sugaya, T. Kawata, N. Ojima, T. Minami, and M. Kawai, Effect of difference of spectral reflectance on appearance of bare skin and cosmetic foundation applied skin, *Proc. AIC'97*, The Color Science Association, Tokyo, Japan, 1997, p. 815.
7. S. Akazaki, M. Zama, N. Inoue, H. Negishi, M. Kawai, and H. Tsutsumi, A relevant study correlating the actual observed physiological properties and a cosmetic-user's subjective evaluations of skin, *J. Soc. Cosmet. Chem. Jpn.* **27**(3), 459 (1993).
8. M. Shimada, Y. Masuda, Y. Yamada, M. Itoh, M. Takahashi, and T. Yatagai, Explanation of human skin color by multiple linear regression analysis based on the modified Lambert–Beer law, **7,** 348 (2000).
9. H. Nakai, Y. Manabe and S. Inokuchi, Simulation and Analysis of Spectral Distributions of Human Skin, *Proc.14th ICPR,* Vol. II,Elsevier, Tokyo, Japan, 1998, p. 1065.
10. M. Okuyama, N. Yokoyama, D. Nakao, N. Tsumura, and Y. Miyake, Accurate mapping pigmentatio ns in human skin by spatio-temporal modulation of light source in the multispectral imaging, *Proc. IS&T's 2003 PICS Conference*, IS&T. Springfield, VA, 2003, p. 272.
11. N. Tsumura, N. Ojima, K. Sato, M. Shiraishi, H. Shimizu, H. Nabeshima, S. Akazaki, K. Hori, and Y. Miyake, Image-based skin color and texture analysis/synthesis by extracting hemoglobin and melanin information in the skin", SIGGRAPH2003, in press (2003).
12. A. Hyvarinen and E. Oja, A fast fixed point algorithm for independent component analysis, *Neural Comp.* **9**(7), 1483–1492 (1997).
13. G. Burel, Blind separation of sources: a nonlinear neural algorithm, *IEEE Trans. Neural Networks* 5, 937 (1992).
14. J. Karhunen, E. Oja, L. Wang, R. Vigario, and J. Joutensalo, A class of neural networks for independent component analysis, *IEEE Trans. Neural Network* **8,** 486 (1997).
15. C. Jutten and J. Hearult, Separation of sources, *Signal Process.* **24**(1), 1 (1991).
16. S. Shafer, Using color to separate reflection components, *Color Res. Appl.* **10**(4), 210–218 (1985).
17. N. Ojima, T. Minami and M. Kawai, Transmittance measurement of cosmetic layer applied on skin by using image processing, *Proc. The 3rd Scientific Conference of the Asian Societies of Cosmetic Scientists*, Allured Publishing Corporation, Carol Stream, IL, 1997, p. 114.
18. N. Tsumura, H. Haneishi and Y. Miyake, Independent component analysis of skin color image, *J. Opt. Soc. Amer. A* **16**(9) 2169–2176 (1999).
19. M. Hiraoka, M. Firbank, M. Essenpreis, M. Cope, S. R. Arrige, P. V. D. Zee, and D. T. Delpy, A Monte Carlo investigation of optical path length in inhomogeneous tissue and its application to near-infrared spectroscopy, *Phys. Med. Biol.* **38,** 1859–1876 (1993).
20. M. S. Drew, C. Chen, S. D. Hordley, and G. D. Finlayson, Sensor transforms for invariant image enhancement, *Proc. IS&T/SID's 10th Color Imaging Conference*,IS&T. Springfield, VA, 2002, pp. 325–330.
21. I. M. Freefberg, A. Z. Eisen, K. Wolff, F. K. Austen, L. A. Goldsmith, S. I. Katz, and T. B. Fitspatrick, 1999 Fitzpatrick's Dermatology in General Medicine, McGraw Hill, New York, New York, 1999.
22. H. Shimizu, K. Uetsuki, N. Ojima, N. Tsumura, and Y. Miyake, Analyzing the effect of cosmetic essence by independent component analysis for skin color images, *Proc. 3rd International Conference on Multispectral Color Science*, University of Joensuu, Joensuu, Finland, 2001, p. 65.

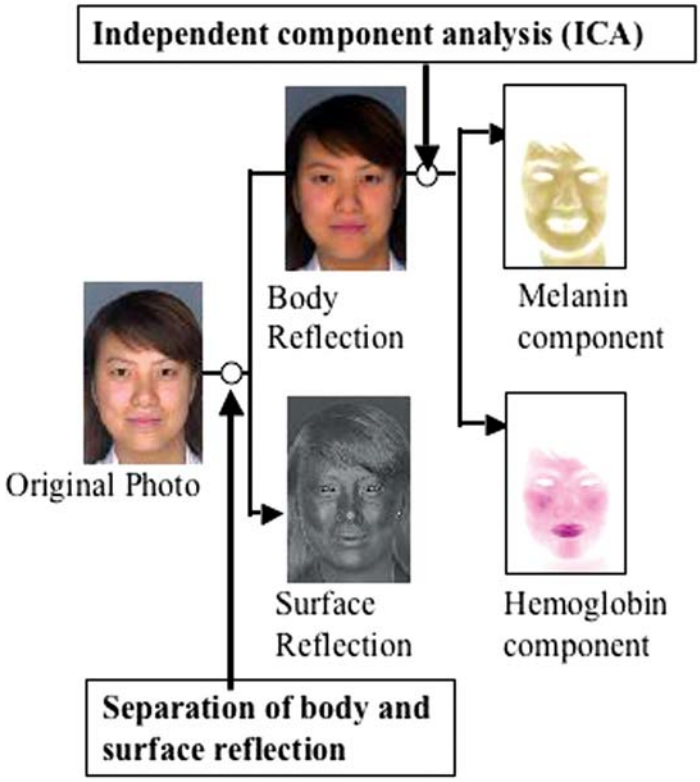

Color Plate 2. Schematic flow of imaging process in the image-based skin color analysis. (*Ojima, et al.,* pp. 222–226)

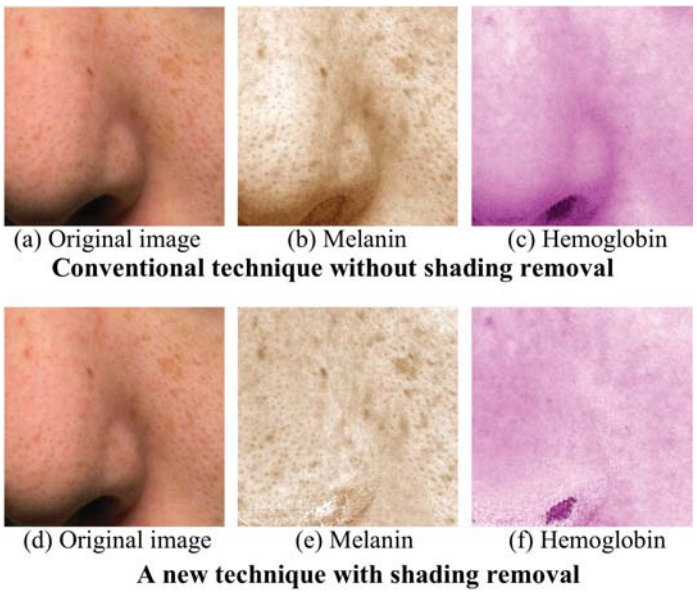

Color Plate 3. The result of independent component analysis with and without shading . (*Ojima, et al.,* pp. 222–226)

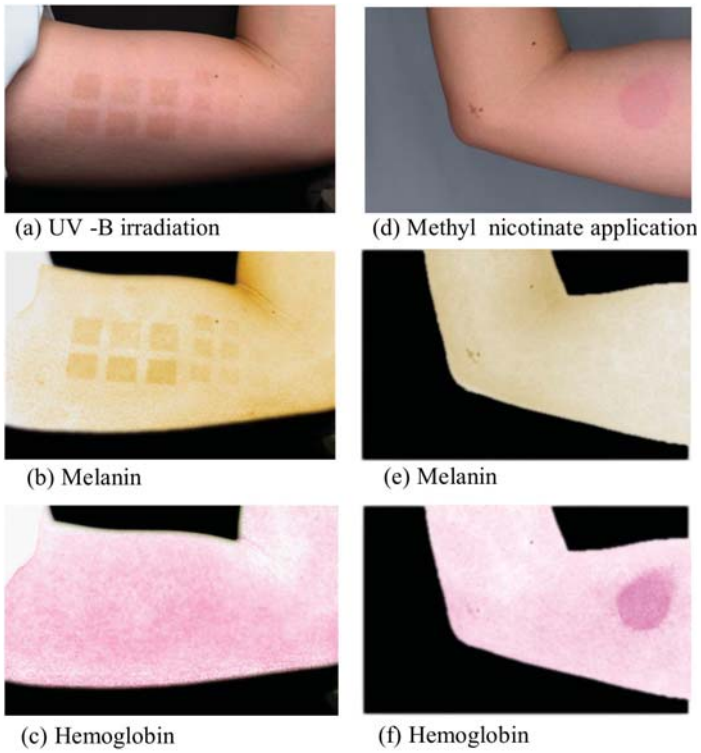

Color Plate 4. Analysis of chromophore patterns generated by artificial treatments. UV-B irradiation: (a) original, (b) melanin component, and (c) hemoglobin component. Application of methyl nicotinate: (d) original, (e) melanin component, and (f) hemoglobin component. (*Ojima, et al.,* pp. 222–226)

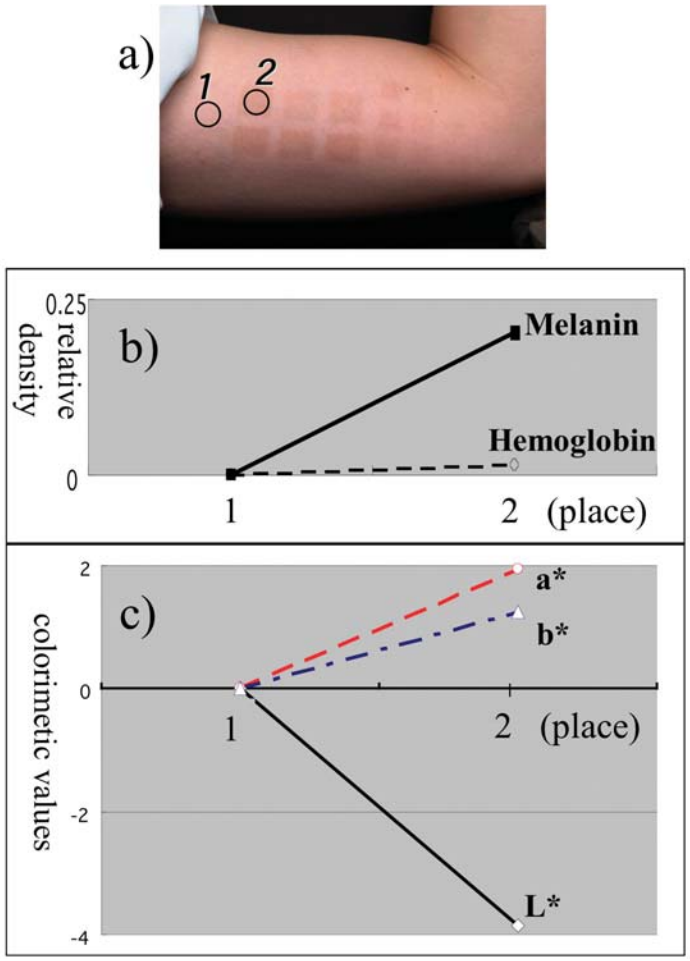

Color Plate 5. Changes of relative chromophores density in accordance with UV-B irradiation. (a) Analyzed two regions of a forearm with and with out irradiation of UV-B (regions no. 1 and no. 2 respectively); (b) relative of chromophore densities between the two regions; and (c) relative colorimetric values in CIEL*a*b* between two regions. (*Ojima, et al.,* pp. 222–226)

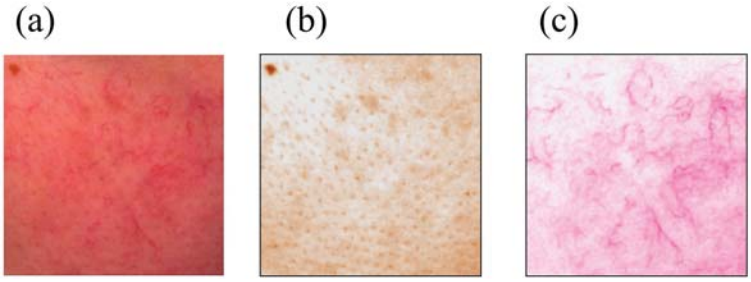

Color Plate 6. Analysis of blood congestion on actual facial skin: (a) original image, (b) melanin component, and (c) hemoglobin component. (*Ojima, et al.,* pp. 222–226)

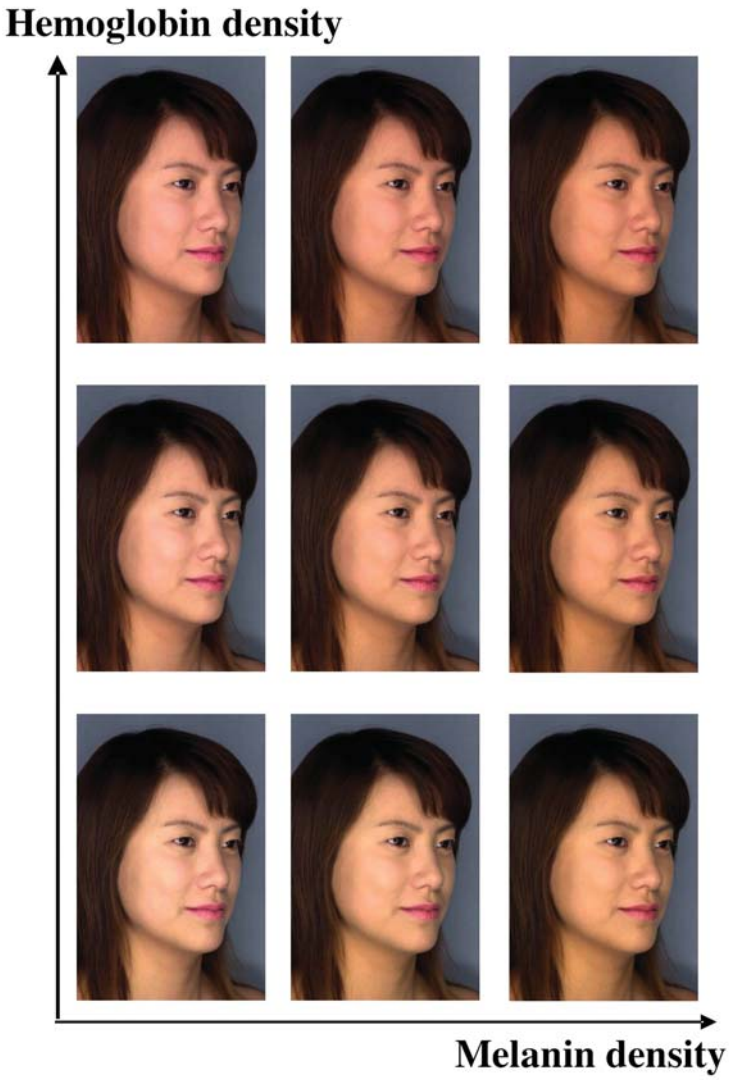

Color Plate 7. Skin color synthesis with changes in melanin and hemoglobin densities (see text). (*Ojima, et al.,* pp. 222–226)